



1

2 *Water Resources Research*

3 Supporting Information for

4 **Abundance and morphometry changes across a high mountain lake-size**
5 **gradient in the tropical Andes of Southern Ecuador**

6 **Pablo V. Mosquera^{1,2}, Henrietta Hampel^{3,5}, Raúl F. Vázquez^{4,5}, Miguel**
7 **Alonso², Jordi Catalan⁶**

8

9 ¹Subgerencia de Gestión Ambiental de la Empresa Pública Municipal de Telecomunicaciones, Agua potable,
10 Alcantarillado y Saneamiento (ETAPA EP), Cuenca, Ecuador.

11 ²Departament de Biologia Evolutiva, Ecologia i Ciències Ambientals, Universitat de Barcelona, Barcelona, Spain.

12 ³Facultad de Ciencias Químicas, Universidad de Cuenca (UC), Ecuador.

13 ⁴Facultad de Ingeniería, UC, Ecuador.

14 ⁵Laboratorio de Ecología Acuática: Departamento de Recursos Hídricos y Ciencias Ambientales, UC, Ecuador.

15 ⁶CREAF-CSIC, Campus UAB, Cerdanyola del Vallès, Spain.

16

17

18 **Contents of this file**

19 **Text S1.** Digital bathymetry method

20 **Figure S1.** Process followed to define the digital bathymetry of the studied lakes

21 **Figure S2.** Altitudinal distribution of the high-mountain lakes of the Cajas Massif

22 **Figure S3.** Some examples of lake shapes and their corresponding shoreline
23 development (D_L)

24 **Figure S4** The relationship between area and volume for the lakes of the Cajas Massif
25 distinguishing two lake morphologies

26 **Figure S5.** Distribution of the maximum depth (Z_{\max}), mean depth (Z_{mean}) and relative
27 depth (Z_r) among the Cajas National Park lakes.

28 **Table S1.** Cajas National Park lakes included in the bathymetry survey

29 **Introduction**

30 The details of the digital bathymetry methods are provided in **Text S1**, and **Figure S1** and the
31 lakes covered by the bathymetry survey in the Cajas National Park are listed in **Table S1**. Four
32 more figures supporting the main text are also included. **Figure S2** shows the altitudinal
33 distribution of the high mountain water bodies of the Cajas Massif. **Figure S3** illustrates some
34 lake shapes across the shoreline development (D_L) gradient. **Figure S4**, the volume-area
35 relationship considering two lake morphologies. And, **Figure S5**, the maximum depth
36 (Z_{\max}), mean depth (Z_{mean}) and relative depth (Z_r) distribution among the Cajas National
37 Park lakes.

38 **Text S1. Digital bathymetry method**

39

40 The process to produce the digital bathymetry of the studied lakes and the derived
41 geomorphological products included: (i) in-situ gathering and office processing of the
42 surveying data so that any incongruence could be filtered out; (ii) preparing the information
43 with the right digital format for the forthcoming steps; (iii) selecting and applying an
44 interpolation algorithm to obtain the bathymetric surface (i.e. the digital bathymetric model)
45 of every surveyed lake; and (iv) obtaining the required geomorphological products derived
46 from the digital bathymetric models of the lakes. For most of these processes, specific-task
47 subroutines were programmed, particularly with PERL (Practical Extracting and Reporting
48 Language) and Matlab®.

49 The first step included the integration of the depth data collected in the field with the
50 data derived from the digitalization of the orthophotos (i.e. boundaries of the lakes associated
51 with zero-depth) so that the feasible bounds of the following interpolation process could be
52 defined properly (besides adding additional zero-depth data for the interpolation process). For
53 filtering out some potential pitfalls of the data collected in the field, these lake boundaries as

54 well as other relevant spatial information, together with field annotations, were contrasted
55 with the aid of geographical information systems (GIS) (ArcGis® and IDRISI® Selva).

56 In the second step, suitable specific-task subroutines, usually programmed with PERL,
57 were used so as to get the different data saved with the right format, as a function of the
58 software that was used later for the interpolation process, particularly Surfer® 13.0.

59 The third step was obtaining the digital bathymetric model of the surveyed lakes. It
60 included assessing an appropriate interpolation algorithm for the current study, by judging
61 the depth accuracy of the resulting interpolation product (i.e. the bathymetric model of a
62 given lake).

63 For some of the studied lakes, the implemented quality assessment process considered a
64 visual comparison (Figure S1) of the results of the different alternative interpolation methods.
65 Through this visual analysis, some of the methods were already discarded. In a second
66 approach, similarly to what is typically done in topographic studies (Vázquez and Feyen, 2007),
67 the accuracy assessment was based on the comparison of the depths modelled with a set of
68 field observations (quality control data set), selected randomly from the set of total field
69 observations. It is important to note that the data of this randomly selected set of observations
70 were not included in the interpolation process itself but, instead, they were only used for
71 quality assessment purposes; that is, only 80 % of the available information was used for
72 deriving the interpolated bathymetric surfaces

73 For a particular interpolation method, the depths comparison was characterised using
74 residuals, that is, the depth difference between the interpolation model and the quality
75 control data set (at the spot locations of these control quality data). This comparison was
76 further aggregated to a single measure depicting the elevation difference between the
77 interpolation product and the quality control data: the Mean Absolute Error (MAE), which is
78 the average of the absolute values of all of the residuals for a particular interpolation product
79 and a particular lake. Absolute values were used to avoid residuals of similar magnitude, but of
80 opposite sign, cancelling to each other, as such, giving the false sensation of low depth
81 discrepancies [Vázquez and Feyen, 2007]. For a particular tested interpolation algorithm, the
82 quality of the method was assessed through a frequency distribution (empirical) function of
83 the MAE, calculated considering the respective interpolation products of all of the studied
84 lakes; so that, the outcome of the quality assessment is a plot of frequency distributions of the
85 MAE as a function of the interpolation method (Figure S1c).

86 In total, ten interpolation methods were tested [Franke and Nielson, 1980; Franke, 1982;
87 Renka, 1988; Hanselman and Littlefield, 1998; Wise, 2000; Vivoni et al., 2005; Vázquez and Feyen,
88 2007; Eldrandaly and Abu-Zaid, 2011], namely, (1) Inverse Distance to a Power, (2) Kriging
89 Standard, (3) Minimum Curvature, (4) Modified Shepard's Method, (5) Natural Neighbour, (6)
90 Nearest Neighbour, (7) Polynomial Regression, (8) Radial Basis Functions, (9) Triangular
91 Interpolation Network (TIN) combined with linear interpolation along the edges of the
92 triangles, and (10) Moving Average.

93 Finally, in the fourth step, the most suitable interpolation method was applied to obtain
94 the digital bathymetric model of each lake surveyed. Given the significant number of lakes
95 considered in the current study, the interpolation and quality control analyses were carried
96 out automatically, using (i) the programming framework that Surfer® enables by mean of
97 Visual Basic; and (ii) PERL specific-purpose subroutines.

98 The outcome of the quality assessment on the products of the ten different interpolation
99 methods considered in this study is depicted in Figure S1c, in the form of ten frequency
100 distribution curves. For a given interpolation method, every dot in the respective distribution
101 curve represents the quality (measured by the MAE) of the bathymetric surface of one of the
102 study lakes obtained by applying the method to the available observations. The figure depicts

103 that indeed these distribution curves enable characterising the differences (and similitudes)
104 among the different interpolation methods since differences (and similitudes) among these
105 curves are systematic. Further, the quality of the products of a given interpolation method,
106 characterized herein by the MAE, shapes the evolution of the respective distribution curve so
107 that better interpolation methods have associated distributions that evolve in a relatively
108 short MAE range, whilst methods that are not that suitable have associated distributions that
109 are spanning (much) longer MAE ranges (Figure S1c).

110 The analysis shows that the best interpolation methods for the conditions of the current
111 study were: (2) Kriging Standard, (3) Minimum Curvature, (5) Natural Neighbour, (6) Nearest
112 Neighbour and (9) TIN with Linear Interpolation, given that the differences among their
113 respective distributions are only marginal and that the associated MAE range is the shortest
114 possible (about 2 m). Thus, we use the Standard version of the Kriging interpolation method
115 for the bathymetry digital development. Nevertheless, statistically, there is not any advantage
116 in using this interpolation method over the other methods with similar MAE distributions in
117 Figure S1c. Indeed, even the simple and traditional (1) Inverse Distance to a Power method
118 performs acceptably compared to methods 2, 3, 5, 6 and 9 (Figure S1c).

119

120 References Text S1

121

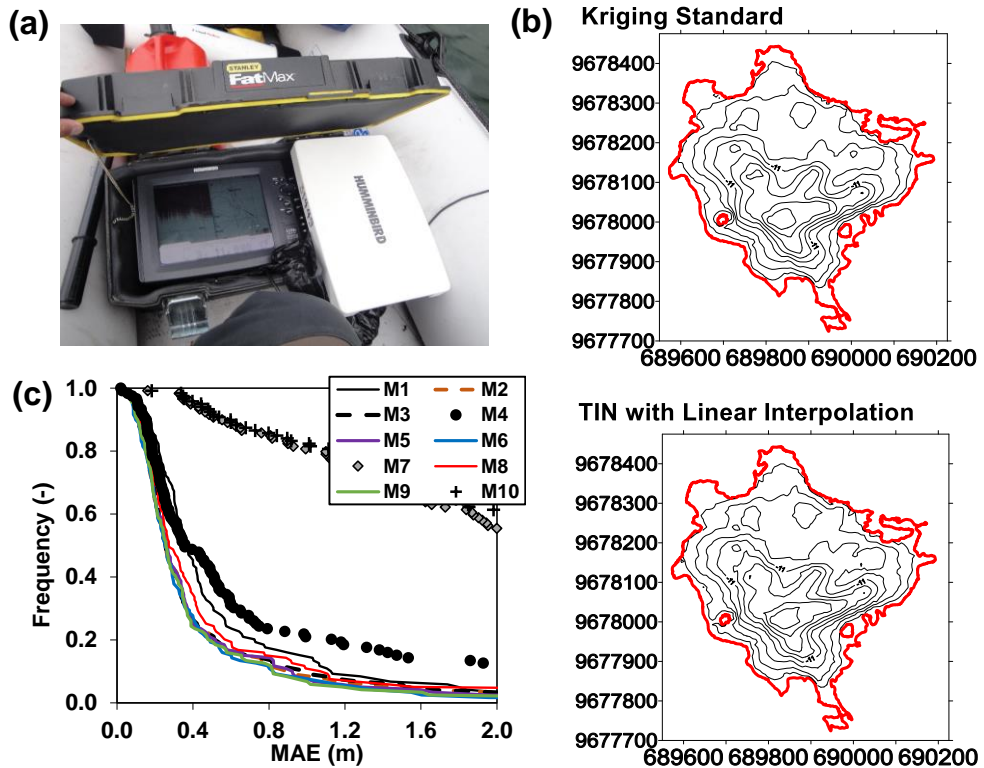
- 122 Eldrandaly, K. A., and M. S. Abu-Zaid (2011), Comparison of six GIS-based spatial
123 interpolation methods for estimating air temperature in Western Saudi Arabia, *J Environ
124 Inform*, 18(1), 38-45.
- 125 Franke, R. (1982), Smooth interpolation of scattered data by local thin plate splines,
126 *Comput Math Appl*, 8(4), 273-281.
- 127 Franke, R., and G. Nielson (1980), Smooth interpolation of large sets of scattered data,
128 *Int J Numer Meth Eng*, 15(11), 1691-1704.
- 129 Hanselman, D., and B. Littlefield (1998), *Mastering MATLAB 5: A Comprehensive
130 Tutorial and Reference*, Prentice-Hall Inc, UK.
- 131 Renka, R. J. (1988), Multivariate interpolation of large sets of scattered data, *ACM Trans
132 Math Softw*, 14(2), 139-148.
- 133 Vázquez, R. F., and J. Feyen (2007), Assessment of the effects of DEM gridding on the
134 predictions of basin runoff using MIKE SHE and a modelling resolution of 600 m, *J
135 Hydrol*, 334(1–2), 73-87.
- 136 Vivoni, E. R., V. Y. Ivanov, R. L. Bras, and D. Entekhabi (2005), On the effects of
137 triangulated terrain resolution on distributed hydrologic model response, *Hydrol Process*,
138 19(11), 2101-2122.
- 139 Wise, S. (2000), Assessing the quality for hydrological applications of digital elevation
140 models derived from contours, *Hydrol Process*, 14(11-12), 1909-1929.

141

142

143

144 **Figure S1.** Process followed to define the digital bathymetry of the studied lakes: (a) sonar
145 used for the surveying; (b) graphical assessment of the quality of the interpolation methods
146 applied on the observed bathymetric data; and (c) statistical evaluation of the quality of the
147 interpolation methods (i.e., frequency distributions of the mean absolute error, MAE, as a
148 function of the interpolation method).

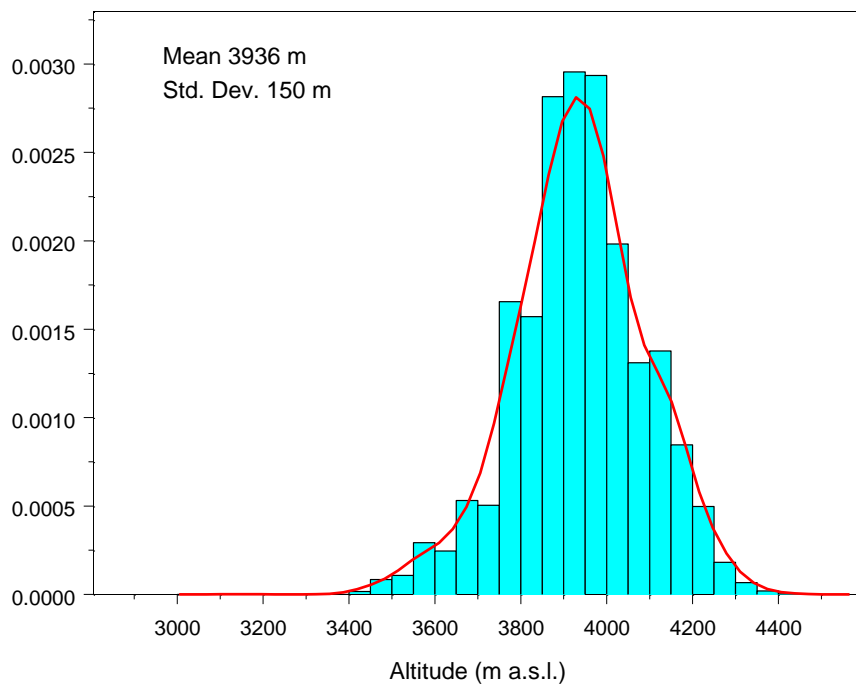


149

150

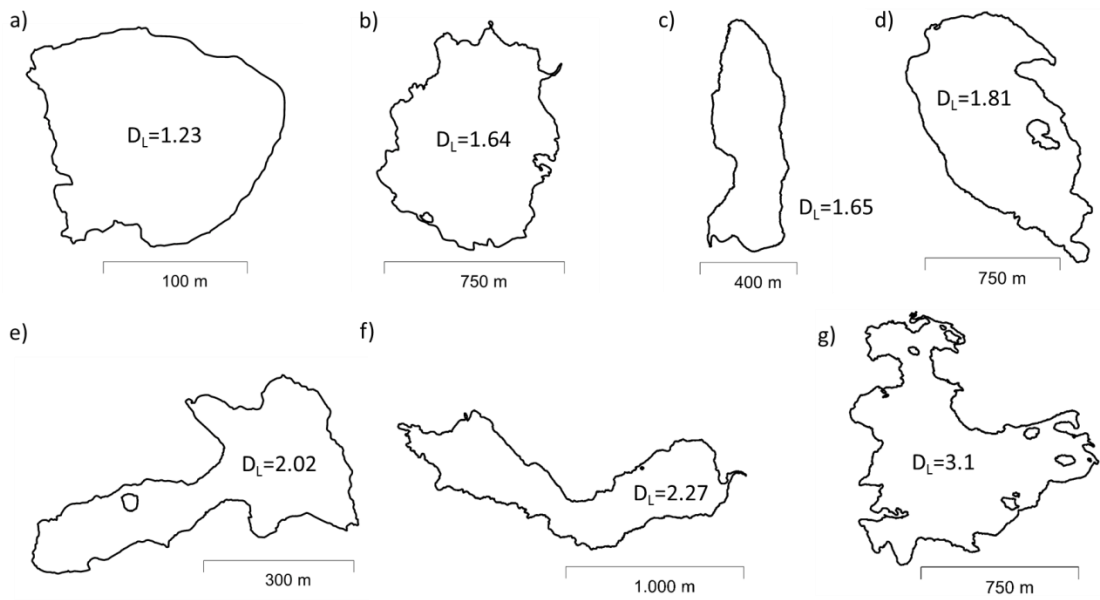
151

152 **Figure S2.** Altitudinal distribution of the high-mountain lakes of the Cajas Massif
153



154
155
156

157 **Figure S3.** Some examples of the lake shapes and their corresponding shoreline development
158 (DL) in the Cajas National Park. a) Laguna de la Cascada , b) Lagartococha , c) Angas , d) Luspa ,
159 e) Burín Grande , f) Mamamag , and g) Osohuayco.
160

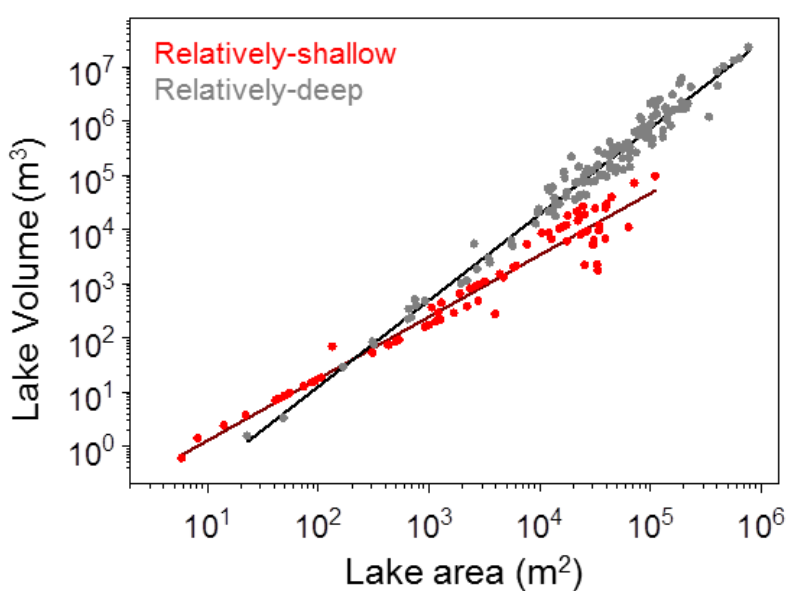


161
162
163
164

165 **Figure S4.** The volume-area relationship for the lakes of the Cajas Massif based on a
166 survey of 202 lakes and ponds in the Cajas National Park and assuming two lake
167 morphologies. The lakes were initially classified into two groups (relatively deep (*rd*)
168 and relatively shallow (*rs*)) according to the positive or negative residuals with respect
169 equation (3) in the main text. Then an allometric equation was fit to each group. The new
170 equations were applied to the whole set, and the lakes were reclassified into two groups
171 according to the lowest residual of the two equations. A new fitting with the new two
172 groups was performed, and then a new reclassification. This procedure was repeated until
173 there were no changes in the classification. The resulting equations were:
174

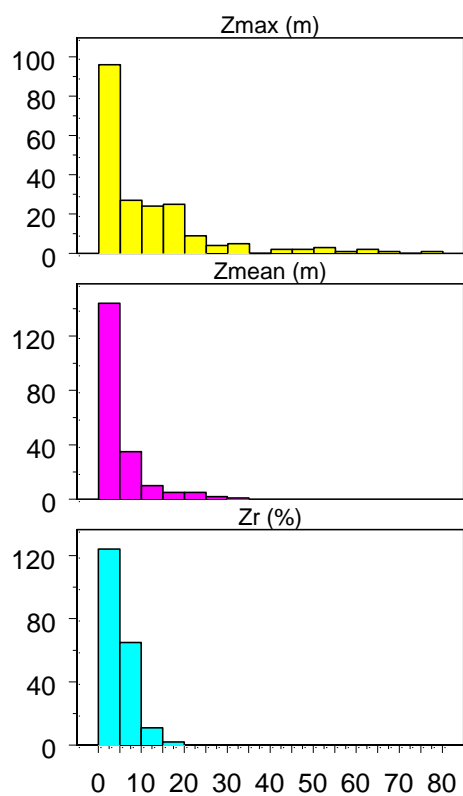
175 $V_{rd} = 0.0084 A_{rd}^{1.59} \quad r^2 = 0.97 \quad n = 130$

176 $V_{rs} = 0.0929 A_{rs}^{1.14} \quad r^2 = 0.96 \quad n = 72$



177
178
179
180
181

182 **Figure S5.** Distribution of the maximum depth (Z_{\max}), mean depth (Z_{mean}) and relative depth
183 (Z_r) among the Cajas National Park lakes.
184



185
186

Table S1 List of the water bodies of the Cajas National Park included in the bathymetry survey

Code	Name	Latitude	Longitude	Altitude (m a.s.l.)
CJ-001	Llaviucu	2° 50' 35.584" S	79° 8' 46.136" W	3152
CJ-002	Patoquinuas	2° 46' 54.316" S	79° 12' 30.998" W	3800
CJ-003	Toreadora	2° 46' 45.871" S	79° 13' 26.144" W	3917
CJ-004	Illincocha	2° 46' 44.674" S	79° 13' 52.401" W	3983
CJ-005	Chica Toreadora	2° 46' 29.042" S	79° 13' 48.313" W	3984
CJ-006	Piñancocha	2° 45' 13.787" S	79° 13' 55.515" W	4221
CJ-007	Fondococha	2° 45' 35.329" S	79° 14' 10.861" W	4127
CJ-008	Pallcacocha	2° 46' 15.057" S	79° 13' 57.561" W	4046
CJ-009	Riñoncocha	2° 45' 58.862" S	79° 13' 46.836" W	4034
CJ-010	Toreador	2° 45' 53.128" S	79° 13' 22.564" W	3927
CJ-011	Ataudcocha	2° 46' 15.415" S	79° 12' 52.294" W	3882
CJ-012	Tintacocha	2° 50' 58.385" S	79° 17' 39.274" W	4033
CJ-013	Del Diablo	2° 50' 39.448" S	79° 17' 45.972" W	4063
CJ-014	Contrahierba	2° 50' 47.165" S	79° 18' 8.754" W	4004
CJ-015	Totorilla	2° 50' 5.796" S	79° 19' 21.697" W	4090
CJ-016	Cristales	2° 50' 27.292" S	79° 19' 5.25" W	4148
CJ-017	Yanacocha de Jerez	2° 50' 18.087" S	79° 19' 33.27" W	4159
CJ-018	Yantahuico 1	2° 50' 0.697" S	79° 20' 37.242" W	4075
CJ-019	Yantahuico 2	2° 50' 4.024" S	79° 20' 19.202" W	4110
CJ-020	Yantahuico 3	2° 50' 16.909" S	79° 20' 14.198" W	4112
CJ-021	Marmolcocha	2° 46' 53.399" S	79° 13' 9.881" W	3926
CJ-022	Unidas	2° 46' 17.781" S	79° 13' 7.02" W	3861
CJ-023	Atugyacu Grande	2° 50' 26.725" S	79° 18' 12.249" W	3969
CJ-024	Estrellascocha	2° 51' 8.014" S	79° 20' 31.706" W	4128
CJ-025	Negra de Jerez	2° 51' 19.484" S	79° 19' 9.092" W	4045
CJ-026	Atascaderos	2° 51' 20.023" S	79° 19' 21.913" W	4038
CJ-027	Pailacocha de Jerez	2° 51' 39.945" S	79° 19' 42.445" W	3970
CJ-028	Atugloma	2° 51' 31.146" S	79° 18' 52.109" W	4141
CJ-029	Angas	2° 52' 1.014" S	79° 17' 56.213" W	3886
CJ-030	Dublaycocha	2° 51' 36.005" S	79° 17' 51.749" W	3915
CJ-031	S/N	2° 52' 11.2" S	79° 17' 32.173" W	4023
CJ-032	Estrellascocha	2° 54' 47.902" S	79° 15' 13.615" W	3818
CJ-033	Lagunaloma o Verdecocha	2° 53' 12.162" S	79° 18' 27.871" W	3837
CJ-034	Napalé Vía	2° 53' 38.702" S	79° 17' 28.384" W	3945
CJ-035	Tinguercocha 1	2° 53' 11.919" S	79° 17' 34.608" W	3895
CJ-036	Ingacasa	2° 51' 31.179" S	79° 16' 19.544" W	3977
CJ-037	Ingacocha 1	2° 51' 39.453" S	79° 16' 1.497" W	3958
CJ-038	Chachacomes	2° 51' 18.704" S	79° 15' 54.082" W	4000

CJ-039	Larga	2° 47' 41.422" S	79° 14' 40.103" W	3940
CJ-040	Negra	2° 47' 0.622" S	79° 14' 33.915" W	4043
CJ-041	Cardenillo	2° 46' 56.252" S	79° 14' 49.979" W	4104
CJ-042	Togllacocha	2° 48' 0.985" S	79° 14' 59.984" W	3859
CJ-043	Luspa	2° 48' 17.395" S	79° 15' 45.61" W	3776
CJ-044	Tinguercocha 2	2° 53' 10.185" S	79° 17' 50.735" W	3888
CJ-045	Cucheros	2° 47' 34.028" S	79° 12' 7.595" W	3887
CJ-046	Canutillos Grande	2° 49' 10.558" S	79° 15' 25.102" W	3851
CJ-047	Canutillos chica 2	2° 49' 50.577" S	79° 15' 9.534" W	3942
CJ-048	Canutillos chica 1	2° 49' 40.139" S	79° 15' 17.255" W	3934
CJ-049	Osohuayco	2° 49' 48.808" S	79° 13' 37.361" W	3856
CJ-050	Mamamag / Taitachugo	2° 49' 44.619" S	79° 11' 38.063" W	3543
CJ-051	Sunincocha Grande	2° 49' 49.679" S	79° 17' 7.03" W	3842
CJ-052	Burín Grande	2° 48' 28.58" S	79° 12' 44.938" W	3891
CJ-053	Burín Chico 1	2° 48' 38.229" S	79° 12' 53.017" W	3872
CJ-054	Burín Chico 2	2° 48' 19.537" S	79° 13' 10.69" W	3900
CJ-055	El Ocho	2° 47' 57.211" S	79° 12' 52.691" W	3991
CJ-056	3ra de Sunincocha	2° 49' 21.461" S	79° 17' 33.718" W	3808
CJ-057	Las Chorreras	2° 49' 12.401" S	79° 17' 5.563" W	4079
CJ-058	2da de Sunincocha	2° 49' 7.169" S	79° 17' 55.949" W	3768
CJ-059	Quinuascocha	2° 50' 15.991" S	79° 16' 6.997" W	3894
CJ-060	Potro muerto	2° 50' 6.73" S	79° 16' 18.343" W	3897
CJ-061	Culebrillas	2° 49' 45.304" S	79° 16' 37.056" W	3955
CJ-062	Cueva Escrita	2° 50' 49.7" S	79° 16' 16.724" W	4019
CJ-063	Llipus loma	2° 50' 59.438" S	79° 15' 58.223" W	4023
CJ-064	Llipus loma 3	2° 50' 38.607" S	79° 16' 22.342" W	4001
CJ-065	Llipus loma 2	2° 50' 42.737" S	79° 16' 19.293" W	4007
CJ-066	Negra	2° 47' 29.339" S	79° 14' 57.895" W	3973
CJ-067	Azul	2° 47' 17.374" S	79° 14' 46.225" W	4043
CJ-068	Pampeada Grande	2° 46' 4.85" S	79° 15' 56.877" W	4121
CJ-069	Pampeada Chica	2° 45' 55.309" S	79° 16' 17.643" W	4158
CJ-070	Del Rayo	2° 46' 7.585" S	79° 16' 19.826" W	4149
CJ-071	Cuchichaspana	2° 50' 14.266" S	79° 15' 45.534" W	3962
CJ-072	Cuchichaspana Chica	2° 50' 25.562" S	79° 14' 37.626" W	3972
CJ-073	Piedra Blanca o Llaviucu	2° 50' 14.636" S	79° 15' 35.834" W	3950
CJ-074	Ojo de Osohuaco	2° 50' 10.497" S	79° 13' 42.055" W	3878
CJ-075	Patos Colorados	2° 50' 12.043" S	79° 13' 10.648" W	3946
CJ-076	Lagartococha	2° 51' 20.322" S	79° 13' 40.233" W	4001
CJ-077	Anexo Osohuayco	2° 50' 0.759" S	79° 13' 39.253" W	3871
CJ-078	Ingacocha 2	2° 51' 40.377" S	79° 16' 10.206" W	3959
CJ-079	J	2° 52' 0.997" S	79° 15' 57.288" W	3919
CJ-080	Martillo	2° 51' 16.491" S	79° 16' 16.199" W	3977
CJ-081	Apicocha 1	2° 47' 14.254" S	79° 12' 40.874" W	3924

CJ-082	Apicocha 2	2° 47' 9.61" S	79° 12' 48.133" W	3924
CJ-083	Apicocha 3	2° 47' 3.046" S	79° 12' 55.88" W	3916
CJ-084	Cascarilla 1	2° 52' 0.094" S	79° 16' 45.694" W	4008
CJ-085	Cascarilla 2	2° 51' 49.49" S	79° 16' 51.182" W	4002
CJ-086	Cascarilla 3	2° 52' 34.23" S	79° 16' 36.48" W	3984
CJ-087	Chica luspa 1	2° 48' 35.76" S	79° 15' 5.145" W	3806
CJ-088	Chica luspa 2	2° 48' 39.979" S	79° 14' 56.106" W	3818
CJ-089	Trensillas	1° 48' 37.684" S	31° 7' 47.755" W	3997
CJ-090	Chullacocha	3° 1' 22.439" S	79° 13' 20.954" W	3787
CJ-091	Quimsacocha 1	3° 3' 12.64" S	79° 14' 43.933" W	3827
CJ-092	Quimsacocha 2	3° 3' 3.29" S	79° 14' 59.297" W	3827
CJ-093	Vado de los Arrieros 1	2° 51' 54.074" S	79° 14' 39.172" W	3814
CJ-094	Vado de los Arrieros 2	2° 51' 25.312" S	79° 14' 49.285" W	3820
CJ-095	Botacocha	2° 51' 38.827" S	79° 14' 31.554" W	3839
CJ-096	Carpahuayco	2° 50' 42.632" S	79° 14' 48.799" W	3917
CJ-097	Jigeno	2° 54' 42.645" S	79° 17' 31.396" W	3969
CJ-098	De Patos	2° 54' 8.287" S	79° 16' 40.515" W	3971
CJ-099	De la Cascada	2° 45' 48.633" S	79° 12' 58.808" W	3967
CJ-100	Cardenillo	2° 45' 25.534" S	79° 12' 46.573" W	4137
CJ-101	Derrumbo Amarillo	2° 45' 52.536" S	79° 12' 35.558" W	4036
CJ-102	Perro Grande	2° 45' 37.052" S	79° 13' 47.775" W	4000
CJ-103	Chica Ventanas	2° 52' 31.268" S	79° 15' 32.668" W	3856
CJ-104	Bejuco	2° 52' 57.996" S	79° 14' 30.203" W	3628
CJ-105	Tintacocha	2° 52' 42.586" S	79° 15' 4.32" W	3679
CJ-106	Ventanas	2° 52' 47.451" S	79° 15' 56.312" W	3913
CJ-107	Chusalongo 1	2° 55' 48.502" S	79° 14' 42.631" W	3778
CJ-108	Chusalongo 2	2° 55' 38.583" S	79° 14' 48.702" W	3794
CJ-109	Chusalongo 3	2° 55' 45.875" S	79° 14' 28.227" W	3780
CJ-110	Chusalongo 4	2° 55' 56.395" S	79° 14' 31.578" W	3764
CJ-111	Del Sharo	2° 46' 1.264" S	79° 16' 38.548" W	4253
CJ-112	Negra	2° 46' 8.977" S	79° 16' 36.627" W	4228
CJ-113	De Patos Blancos	2° 45' 40.312" S	79° 16' 24.755" W	4210
CJ-114	Juan Pasana	2° 45' 30.525" S	79° 16' 33.057" W	4294
CJ-115	Chica Hunanchi	2° 51' 58.855" S	79° 13' 54.419" W	3874
CJ-116	Hunanchi	2° 52' 19.022" S	79° 14' 4.328" W	3834
CJ-117	Verdes	2° 51' 33.277" S	79° 12' 57.346" W	3886
CJ-118	Estrellascocha 2	2° 55' 10.523" S	79° 15' 11.119" W	3769
CJ-119	Estrellascocha 3	2° 55' 4.383" S	79° 14' 58.274" W	3802
CJ-120	Estrellascocha 4	2° 55' 15.687" S	79° 15' 23.674" W	3761
CJ-121	Dos Choreras	2° 46' 12.542" S	79° 9' 36.858" W	3690
CJ-122	Taquiruco	2° 46' 44.076" S	79° 11' 57.279" W	3623
CJ-123	Barros	2° 46' 38.203" S	79° 12' 10.108" W	3815
CJ-124	Charco-Anex-Barros	2° 46' 41.038" S	79° 12' 11.82" W	3824

CJ-125	Humedal Totora	2° 46' 44.464" S	79° 12' 17.448" W	3824
CJ-126	Charco Pardo Anex Humedal	2° 46' 44.174" S	79° 12' 19.358" W	3832
CJ-127	Barros 2	2° 46' 18.392" S	79° 12' 19.624" W	3871
CJ-128	Barros 3	2° 46' 24.609" S	79° 12' 18.675" W	3873
CJ-129	Charca Anexo Barros 3	2° 46' 28.025" S	79° 12' 17.181" W	3863
CJ-130	Charca 2 Anexo Barros 3	2° 46' 28.48" S	79° 12' 17.018" W	3859
CJ-131	Totoras	2° 46' 50.554" S	79° 12' 40.424" W	3810
CJ-132	Verdecocha	2° 48' 54.131" S	79° 9' 35.117" W	3659
CJ-133	San Antonio 1	2° 49' 17.978" S	79° 10' 7.034" W	3846
CJ-134	San Antonio 2	2° 49' 34.423" S	79° 10' 10.925" W	3721
CJ-135	Patococha 1	2° 48' 34.226" S	79° 10' 27.498" W	3841
CJ-136	Charca Anexo Pato 2	2° 48' 21.486" S	79° 10' 19.586" W	3801
CJ-137	Patococha grande 1	2° 48' 22.024" S	79° 10' 9.873" W	3783
CJ-138	Charca Anexo Patococha 1	2° 48' 11.467" S	79° 10' 3.512" W	3754
CJ-139	Lago Anexo Estrellascocha 1	2° 51' 5.881" S	79° 20' 19.729" W	4125
CJ-140	Charca Anexo Estrellascocha 1	2° 51' 9.305" S	79° 20' 23.933" W	4116
CJ-141	Estrellascocha 2	2° 51' 20.09" S	79° 20' 52.508" W	4074
CJ-142	Estrellascocha 3	2° 51' 15.583" S	79° 20' 42.283" W	4092
CJ-143	Estrellascocha 4	2° 51' 19.298" S	79° 20' 45.192" W	4088
CJ-144	Charca Anexo Estrellascocha 4	2° 51' 18.876" S	79° 20' 45.937" W	4095
CJ-145	Lago somero anexo Estrella 2	2° 51' 28.681" S	79° 20' 49.55" W	4073
CJ-146	Estrellas 5	2° 51' 22.036" S	79° 20' 47.034" W	4084
CJ-147	Lago somero anexo Yantahuico 1	2° 50' 7.428" S	79° 20' 31.696" W	4085
CJ-148	Lago somero anexo Yantahuico 4	2° 50' 7.787" S	79° 20' 32.019" W	4086
CJ-149	Cocha totorilla 1	2° 50' 4.336" S	79° 19' 47.213" W	4223
CJ-150	Cocha totorilla 2	2° 50' 4.435" S	79° 19' 48.41" W	4229
CJ-151	Cocha totorilla 3	2° 50' 4.274" S	79° 19' 49.479" W	4232
CJ-152	Cocha totorilla 4	2° 50' 20.934" S	79° 19' 21.351" W	4169
CJ-153	Cocha Jerez 1	2° 51' 23.571" S	79° 19' 21.52" W	4040
CJ-154	Cocha Jerez 2	2° 51' 17.444" S	79° 19' 16.769" W	4029
CJ-155	Cocha Jerez 3	2° 51' 16.337" S	79° 19' 16.35" W	4036
CJ-156	Cocha totorilla 5	2° 49' 46.18" S	79° 19' 31.568" W	4078
CJ-157	Culebrillas	2° 25' 25.25" S	78° 51' 38.535" W	3901
CJ-158	Paredones	2° 25' 36.083" S	78° 51' 35.508" W	3946
CJ-159	Charca anostraceos	2° 47' 2.928" S	79° 14' 51.944" W	4131
CJ-160	Charca L2	2° 47' 2.359" S	79° 14' 41.261" W	4070
CJ-161	Lago somero anexo L2	2° 47' 2.23" S	79° 14' 42.427" W	4071
CJ-162	Lago somero anexo larga	2° 47' 34.331" S	79° 14' 44.257" W	3955
CJ-163	Lago somero anexo luspa	2° 48' 12.803" S	79° 15' 22.306" W	3819
CJ-164	Charca anostraceos 2	2° 48' 1.836" S	79° 15' 46.96" W	3804
CJ-165	AN-CH001	2° 52' 22.047" S	79° 17' 57.639" W	3884
CJ-166	Charca anostraceos anexo angas	2° 52' 22.346" S	79° 18' 1.685" W	3881
CJ-167	Lago Azul	2° 52' 56.986" S	79° 17' 19.412" W	3974

CJ-168	Charca Anexo a tinguercocha 1	$2^{\circ} 53' 10.27''$ S	$79^{\circ} 17' 20.72''$ W	3894
CJ-169	Las Chorreras 2	$2^{\circ} 49' 10.655''$ S	$79^{\circ} 16' 51.806''$ W	4085
CJ-170	Mangacocha 1	$2^{\circ} 49' 52.989''$ S	$79^{\circ} 16' 16.097''$ W	4009
CJ-171	Mangacocha 2	$2^{\circ} 49' 49.301''$ S	$79^{\circ} 16' 10.048''$ W	3995
CJ-172	Mangacocha 3	$2^{\circ} 49' 52.261''$ S	$79^{\circ} 16' 8.619''$ W	4009
CJ-173	Charca SU 1	$2^{\circ} 49' 49.433''$ S	$79^{\circ} 16' 33.294''$ W	3966
CJ-174	1ra de Sunincocha	$2^{\circ} 48' 54.454''$ S	$79^{\circ} 18' 5.195''$ W	3752
CJ-175	Charco 1 anexo Ingacocha 1	$2^{\circ} 51' 19.642''$ S	$79^{\circ} 16' 32.674''$ W	4046
CJ-176	Lago somero 2 anexo a Ingacasa	$2^{\circ} 51' 15.586''$ S	$79^{\circ} 16' 41.519''$ W	4045
CJ-177	Charco 3 anexo a Ingacasa	$2^{\circ} 51' 22.125''$ S	$79^{\circ} 16' 38.693''$ W	4007
CJ-178	Lago somero anexo a Ingacocha 2	$2^{\circ} 51' 42.128''$ S	$79^{\circ} 15' 44.042''$ W	3960
CJ-179	Lago somero 2 anexo a Ingacocha 2	$2^{\circ} 51' 41.357''$ S	$79^{\circ} 15' 50.81''$ W	3975
CJ-180	Lago somero 3 anexo a Ingacocha 2	$2^{\circ} 51' 37.646''$ S	$79^{\circ} 15' 50.654''$ W	3984
CJ-181	Charco 1 anexo a tintacocha	$2^{\circ} 52' 42.367''$ S	$79^{\circ} 12' 23.534''$ W	3705
CJ-182	Hato de Chocar	$2^{\circ} 52' 10.414''$ S	$79^{\circ} 12' 12.123''$ W	3706
CJ-183	Lago somero Hato de Chocar 1	$2^{\circ} 52' 22.521''$ S	$79^{\circ} 12' 9.74''$ W	3703
CJ-184	Totoracocha	$2^{\circ} 52' 55.054''$ S	$79^{\circ} 11' 36.535''$ W	3583
CJ-185	Hato de chocar 2 o Tintacocha	$2^{\circ} 52' 31.435''$ S	$79^{\circ} 12' 26.789''$ W	3968
CJ-186	Chuspihuaycu	$2^{\circ} 51' 36.54''$ S	$79^{\circ} 11' 19.014''$ W	3578
CJ-187	Perro chico	$2^{\circ} 45' 41.136''$ S	$79^{\circ} 13' 36.212''$ W	3950
CJ-188	L-SU1	$2^{\circ} 50' 9.413''$ S	$79^{\circ} 16' 27.404''$ W	3886
CJ-189	LSO2	$2^{\circ} 50' 6.975''$ S	$79^{\circ} 16' 29.739''$ W	3897
CJ-190	L. somero anexo a Culebrillas	$2^{\circ} 49' 42.518''$ S	$79^{\circ} 16' 46.255''$ W	3971
CJ-191	Charco anexo Culebrillas	$2^{\circ} 49' 49.114''$ S	$79^{\circ} 16' 37.762''$ W	3957
CJ-192	Charco anexo Culebrillas	$2^{\circ} 49' 50.548''$ S	$79^{\circ} 16' 38.893''$ W	3953
CJ-193	Charco anexo Osohuayco	$2^{\circ} 50' 0.99''$ S	$79^{\circ} 13' 41.228''$ W	3865
CJ-194	Charco anexo Osohuayco 2	$2^{\circ} 49' 59.753''$ S	$79^{\circ} 13' 41.359''$ W	3867
CJ-195	Charco anexo Osohuayco 3	$2^{\circ} 49' 58.971''$ S	$79^{\circ} 13' 41.166''$ W	3883
CJ-196	Chico Juan Manuel	$2^{\circ} 50' 12.024''$ S	$79^{\circ} 12' 37.171''$ W	3775
CJ-197	Charco anexo Osohuayco 4	$2^{\circ} 49' 59.768''$ S	$79^{\circ} 13' 51.363''$ W	3894
CJ-198	Charco anexo Osohuayco 5	$2^{\circ} 50' 2.587''$ S	$79^{\circ} 13' 42.488''$ W	3866
CJ-199	Atucpamba 1	$2^{\circ} 52' 1.934''$ S	$79^{\circ} 18' 45.685''$ W	4143
CJ-200	Atucpamba 2	$2^{\circ} 51' 55.38''$ S	$79^{\circ} 18' 38.539''$ W	4156
CJ-201	Atucpamba 3	$2^{\circ} 51' 53.233''$ S	$79^{\circ} 18' 40''$ W	4148
CJ-202	Atucpamba 4	$2^{\circ} 51' 47.079''$ S	$79^{\circ} 18' 39.329''$ W	4147